Mapping Drug Interactions at the Covalent Topoisomerase II-DNA Complex by Bisantrene/Amsacrine Congeners*

Giovanni Capranico‡, Fulvio Guano, Stefano Moro§, Giuseppe Zagotto§, Claudia Sissi§, Barbara Gatto§, Franco Zunino, Ernesto Menta¶, and Manlio Palumbo§

From the Division of Experimental Oncology B, Istituto Nazionale per lo Studio e la Cura dei Tumori, via Venezian 1, 20133 Milan, the §Department of Pharmaceutical Sciences, University of Padua, Via Marzolo 5, 35131 Padua, and the ¶Boehringer Mannheim Italia, Research Center, 20052 Monza, Italy

To identify structural determinants for the sequence-specific recognition of covalent topoisomerase II-DNA complexes by anti-cancer drugs, we investigated a number of bisantrene congeners, including a 10-azabioisoster, bearing one or two 4,5-dihydro-1*H*-imidazol-2-yl hydrazone side chains at positions 1, 4, or 9 of the anthracene ring system. The studied bisantrene/amsacrine (*m*-AMSA) hybrid and bisantrene isomers were able to poison DNA topoisomerase II with an intermediate activity between those of bisantrene and *m*-AMSA. Moving the side chain from the central to a lateral ring (from C-9 to C-1/C-4) only slightly modified the drug DNA affinity, whereas it dramatically affected local base preferences of poison-stimulated DNA cleavage. In contrast, switching the planar aromatic systems of bisantrene and *m*-AMSA did not substantially alter the sequence specificity of drug action. A computer-assisted steric and electrostatic alignment analysis of the test compounds was in agreement with the experimental data, since a common pharmacophore was shared by bisantrene, *m*-AMSA, and 9-substituted analogs, whereas the 1-substituted isomer showed a radically changed pharmacophoric structure. Thus, the relative space occupancy and electron distribution of putative DNA binding (aromatic rings) and enzyme binding (side chains) moieties are fundamental in directing the specific action of topoisomerase II poisons and in determining the poison pharmacophore.

The elucidation of structural determinants of the sequence-specific recognition of DNA by small molecules is fundamental for a rational design of gene-specific DNA binders that are effective in the therapy of human diseases. Several DNA-interactive compounds are known that may bind to the double helix in a site-selective manner; however, the degree and mechanisms of the specificity are very different among them (1–4). A wide variety of antitumor drugs, with and without the ability to bind to naked DNA, have been shown to poison DNA topoisomerases with a high sequence selectivity (2, 5–7). DNA topoisomerases are ubiquitous enzymes deputed to resolve topological problems that arise during various nuclear processes including transcription, recombination, and chromosome partitioning at cell division (8–10). Type II enzymes make transient double-stranded breaks into one segment of DNA and pass an intact duplex through the broken DNA, before resealing the break (2, 8–10). Anticancer agents able to poison the mammalian enzymes stabilize a key intermediate of the catalytic reaction wherein DNA strands are broken and covalently linked to the protein. Thus, the poisoning action results in increased DNA cleavage levels in living cells that eventually trigger a cell death process.

Classical topoisomerase poisons stimulate DNA cleavage in a sequence-selective manner, yielding drug-specific cleavage intensity patterns in agarose as well as sequencing gels (2, 5, 6, 11, 12). Each pattern reflects the recognition of specific features of the enzyme-DNA covalent complex that are likely dictated by the nucleotide sequence at the site of cleavage. In fact, while preferred bases distant from the cleaved bond are similar regardless of the class of the poison used (enzyme-specific preferences), preferred nucleotides close to the 5′- or 3′-termini (positions +1 or −1, respectively) are poison-specific, examples being an adenine at +1 for *m*-AMSA[1] and bisantrene, a cytosine at −1 for teniposide (VM-26) and mitoxantrone, an adenine at −1 for doxorubicin, and a thymine at +2 for streptonigrin (2). Poison localization in the ternary complex has been directly shown using a photoactivable *m*-AMSA analog (13). Upon activation, the compound was found to be covalently linked to DNA bases at the +1 and −1 positions, only when T4 topoisomerase II was present in the reaction mixture. Analogous results have been obtained in the case of camptothecin and topoisomerase I (14, 15). Thus, several independent results demonstrate that poison receptors are localized at the protein/DNA interface at the site of DNA cleavage.

Early studies suggested that topoisomerase II poisons may fit into a "loose" pharmacophore, constituted by a planar ring system with DNA intercalation or intercalation-like properties, and one or two protruding side chains, possibly interfering with the protein side of the covalent enzyme-DNA complex (16). The lack of structural restrictions on this pharmacophore can be ascribed mainly to the receptor heterogeneity that is determined by different nucleic acid sequences at the enzyme-active site. An approach to the characterization of the drug receptor site has been based on molecular modeling analyses of topoisomerase II poisons along with the determination of their sequence-specific DNA cleaving activity (17). The relative positions of planar ring systems and side chains of many clinically useful antitumor topoisomerase II poisons have been suggested to determine the site of enzyme-mediated DNA cleavage (17).

† To whom reprint requests should be addressed: Istituto Nazionale Tumori, Experimental Oncology B, 20133 Milan, Italy. Tel.: 39-2-2390-203; Fax: 39-2-2390-764; E-mail: capranico@istitutotumori.mi.it.

[1] The abbreviations used are: *m*-AMSA, amsacrine, 4-[9-acridinylamino]-*N*-[methanesulfonyl]-*m*-anisidide; IHA, dihydro-1*H*-imidazol2-yl hydrazone; SEA, steric and electrostatic analysis; NOE, nuclear Overhauser effect.

As a matter of fact, only compounds sharing defined steric and electronic features can trap the enzyme at the same DNA sites. In particular, bisantrene and *m*-AMSA have the same base preference for DNA cleavage stimulation, and despite the different chemical structures, they were shown to be characterized by very similar electronic and steric properties, suggesting a common fit into the receptor site (17).

Therefore, in order to challenge the idea that the drug shape and electron density determine the sequence specificity of the poison action, bisantrene analogs and an *m*-AMSA-bisantrene hybrid (Fig. 1) were synthesized and characterized for their DNA binding properties, topoisomerase II-mediated DNA cleavage, base sequence preferences, and conformational and electronic features. The studied compounds were formally derived from the exchange of putative pharmacophoric domains of *m*-AMSA and bisantrene or were structural isomers of bisantrene (Fig. 1). In full agreement with the original hypothesis, our combined experimental and theoretical work demonstrates that alterations of the shape and electron density of the drug molecule markedly affect the sequence-specific interaction of the poison with topoisomerase II-DNA complexes. This might be useful in providing a physicochemical map of poison receptors.

EXPERIMENTAL PROCEDURES

Materials—*m*-AMSA and bisantrene were obtained by the Drug Synthesis and Chemistry Branch, NCI, National Institutes of Health, Bethesda, and by Lederle, Copenhagen, Denmark, respectively. The IHA compounds were synthesized as described and characterized previously (18). All the compounds used were stored at $-20\,°C$ in Me_2SO or deionized water and diluted in deionized water prior to use. DNA from calf thymus ($\epsilon = 6600\ M^{-1}\ cm^{-1}$), was purchased from Sigma and used with no further purification. DNA topoisomerase II was purified from nuclei of murine P388 leukemia cells and stored as described (19). Human topoisomerase IIα was purified from yeast cells carrying a plasmid-borne human top2α cDNA, as described already (20). Simian virus 40, restriction endonucleases, other enzymes, agarose, and acrylamide were from Life Technologies, Inc., or from New England Biolabs. $[\gamma\text{-}^{32}P]ATP$ was from Amersham Pharmacia Biotech (Milan, Italy).

DNA Binding Studies—Measurements were carried out in 10 mM Tris-HCl, pH 7.0, 1 mM EDTA, 0.15 M NaCl at 25 °C. Binding was followed spectrophotometrically or fluorometrically in the ligand absorption or emission region upon adding scalar amounts of DNA to a freshly prepared drug solution. To avoid large systematic inaccuracies due to experimental errors in extinction coefficients or fluorescence quantum yield, the range of bound drug fractions was 0.15–0.85. Data were evaluated according to Equation 1 of McGhee and Von Hippel for non-cooperative ligand-lattice interactions (21),

$$r/m = K_i(1 - nr)^n/[1 - (n - 1)r]^{n-1}, \qquad \text{(Eq. 1)}$$

where *r* is the molar ratio of bound ligand to DNA; *m* is the free ligand concentration; K_i is the intrinsic binding constant; and *n* is the exclusion parameter. Spectrophotometric measurements were performed with a Perkin-Elmer Lambda 5 apparatus and fluorometric studies on a MPF66 fluorometer, both equipped with a Haake F3-C thermostat.

Topoisomerase II-mediated DNA Cleavage—SV40 DNA was linearized with a restriction enzyme, treated with calf intestinal phosphatase, and uniquely 5′-end-labeled using T4 polynucleotide kinase and $[\gamma\text{-}^{32}P]ATP$ prior to digestion with a second endonuclease (11). Labeled DNA was incubated for 20 min at 37 °C with topoisomerase II (10–30 units) with or without drugs in 40 mM Tris-HCl, pH 7.5, 0.5 mM dithiothreitol, 100 mM NaCl, 10 mM MgCl$_2$, 1 mM ATP, 15 μg/ml bovine serum albumin, and 1% Triton X-100. The presence of the surfactant reduces the extent of DNA-protein aggregation that would otherwise affect drug-stimulated DNA cleavage (22). Reactions were stopped by incubation with 1% SDS and 0.1 mg/ml proteinase K for 45 min at 42 °C. Samples were then electrophoresed in a 1% agarose gel in 89 mM Tris, 89 mM boric acid, 2 mM EDTA, pH 8, and 0.1% SDS. For sequencing gels, after proteinase K treatment, DNA was ethanol-precipitated, resuspended in 80% formamide, 10 mM NaOH, 1 mM EDTA, 0.1% dyes, heated for 2 min at 90 °C, chilled on ice, and loaded onto a 8% poly-

acrylamide denaturing gel. Gels were run for 2 h at 70 watts, dried, and autoradiographed to Amersham Hyperfilms (Amersham Pharmacia Biotech). The reduction of the full-length labeled DNA band was used to measure drug stimulation or suppression of enzyme-mediated DNA cleavage. The level of radioactivity of the uncut DNA band in each lane was quantified by volume integration using the ImageQuant program on a Molecular Dynamics PhosphorImager 425 model.

Statistical Analysis of Cleavage Site Specificity—Poison-stimulated DNA cleavage sites were mapped by comparison with Maxam-Gilbert purine markers (11). The collected site sequences were gathered into drug-specific groups, and base frequencies at each position around the cleaved bonds were analyzed by using statistical tests as described in detail elsewhere (11, 17, 23).

Computational Chemistry—Ab initio calculations were performed at Hartree-Fock level with Gaussian basis set 3–21G(*) (24). All geometries were fully optimized without geometry constraints. Vibrational frequency calculations were used to characterize the minima stationary points (zero imaginary frequencies). The software package Spartan 3.1 (Wavefunction Inc., Irvine, CA) was used for all quantum mechanical calculations. The optimized geometry and the atomic charges allowed us to perform a steric and electrostatic analysis (SEA) (25). For this purpose, the Superimposition/Similarity facility to Spartan 4.0 (Wavefunction Inc., Irvine, CA) was employed for the alignment of molecular structures. Optimized alignments were achieved by maximizing the electrostatic potential field and steric overlap of three-dimensional structures. This method performs the alignment many times for a single pair of molecules and keeps only the best results, which are finally sorted according to a functional form of the similarity measure. The functional forms were generated as three-dimensional grids surrounding each molecule to analyzed. In this work a correlation coefficient (*r*), as shown in Equation 2, was used as a similarity index,

$$r = \frac{n\sum_i x_i y_i - (\sum_i x_i)(\sum_i y_i)}{[(n\sum_i x_i^2 - (\sum_i x_i)^2)(n\sum_i y_i^2 - (\sum_i y_i)^2)]^{1/2}}, \qquad \text{(Eq. 2)}$$

where *n* is the grid number and x_i, y_i the corresponding coordinates (26). All molecular modeling calculations were performed on an IBM RISC System 6000 model 250 Unix workstation.

NMR Experiments—Nuclear Overhauser (NOE) experiments were performed in deuterated chloroform using a Varian Gemini 300 MHz spectrometer. To freeze drug conformations, the temperature was reduced to $-50\,°C$ in a number of runs. Since, as expected, the relevant structural information could be obtained from the data concerning the imine proton, this has been especially considered in the NOE spectra.

RESULTS

Drug Stimulation of DNA Cleavage—Levels of topoisomerase II-dependent DNA cleavage in the presence of the studied compounds (Fig. 1) were determined in 5′-end ^{32}P-labeled SV40 DNA fragments by PhosphorImager analysis of agarose gels. With the exception of 1,4-IHA, the new compounds stimulated DNA cleavage mediated by murine native enzyme and recombinant human topoisomerase IIα (Fig. 2). The parent drugs *m*-AMSA and bisantrene were the most and the least active compounds, respectively. 9-IHA stimulated intermediate cleavage levels; 1-IHA stimulated a low level of cleavage only at 10 μM, and aza-9-IHA was as active as bisantrene (Fig. 2). Potency was also reduced for all the new analogs, since cleavage was detectable at 1–10 μM, whereas bisantrene and *m*-AMSA stimulated cleavage at 0.2–1 μM (Figs. 3 and 4). No cleavage suppression was detected up to 10 μM of the analogs and *m*-AMSA, in contrast to bisantrene that at the same concentration suppressed even background cleavage. 1,4-IHA was completely ineffective and abolished enzyme-mediated DNA cleavage even at 0.1 μM (Figs. 2 and 3). This is likely due to the high DNA binding affinity constant and precipitation of drug-nucleic acid aggregates (see below).

Cleavage Intensity Patterns with Murine Native Topoisomerase II and Human Topoisomerase IIα Form—To compare drug-stimulated cleavage patterns, topoisomerase II-dependent
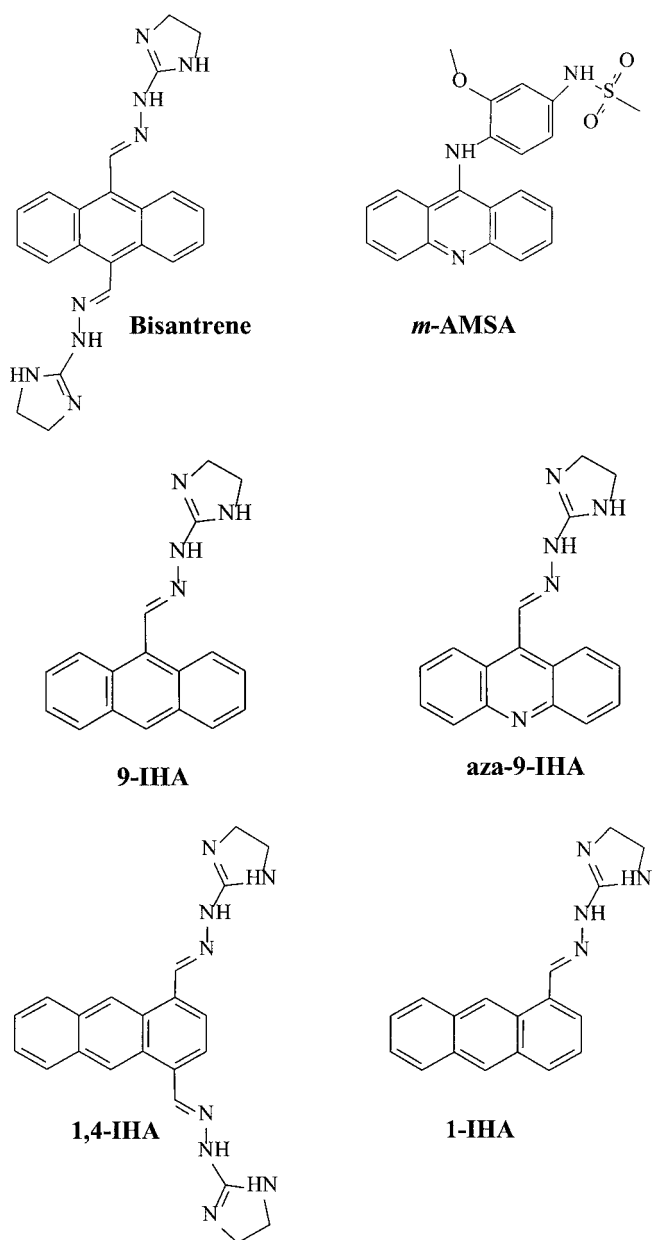
FIG. 1. **Chemical structures of the studied compounds.**

FIG. 2. **Levels of topoisomerase II DNA cleavage by *m*-AMSA/bisantrene congeners.** An SV40 DNA fragment, ^{32}P-labeled at the 5′-end of the *Bam*HI site, was incubated with topoisomerase II and poisons at 37 °C for 20 min. Reactions were stopped with SDS (1%) and proteinase K (0.1 mg/ml). DNA cleavage was then examined by 1% agarose gel electrophoresis, and cleavage levels were determined with PhosphorImager analyses. Numbers *above* columns indicate the stimulation (above 1) or suppression (below 1) factor, calculated as the ratio of the cleaved DNA fraction with the drug over that without drugs.

DNA cleavage was further investigated with sequencing gels. Intensity cleavage patterns of 9-IHA, aza-9-IHA, and *m*-AMSA were somewhat different even though many cleavage sites were common (Figs. 3 and 4). This is shown by cleavage stimulation with murine native topoisomerase II at the genomic positions 2401, 2430, 2438, 2441, and 2465 (Fig. 3*A*; see also sites indicated by *arrowheads* in Fig. 3*B*). In contrast, 1-IHA stimulated cleavage at a different subset of sites (genomic positions 2408, 2445, 2447, and the *asterisk* in Fig. 3). Some sites stimulated by 1-IHA were also stimulated by 9-IHA but not by *m*-AMSA and aza-9-IHA (Fig. 3, *sites 2447* and *2408*). However, these sites were a minor fraction of all the sites stimulated by 9-IHA.

Drug-stimulated DNA cleavage was also investigated with human recombinant topoisomerase IIα in the region of the SV40 replication origin (Fig. 4). IHA congeners stimulated main cleavage sites in the purine/pyrimidine repeats within the 72-base pair repeats of SV40 DNA. Again sites stimulated by the congeners (see *sites 263, 204, 200,* and *142*, in Fig. 4) were also sites of *m*AMSA-stimulated DNA cleavage. However,
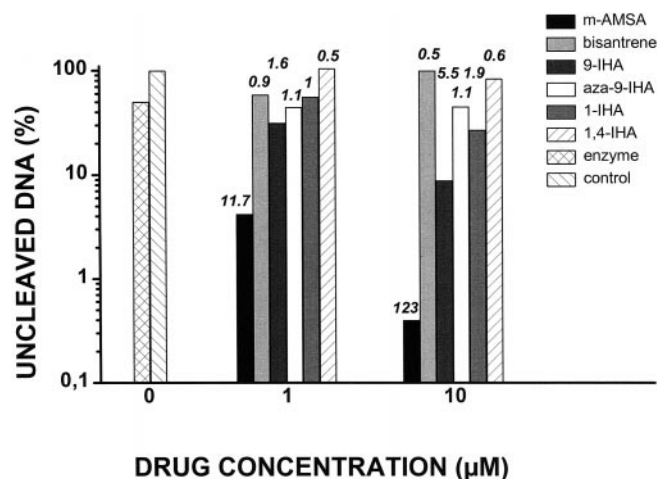
other main amsacrine sites (see *sites 252, 241, 223* and others in Fig. 4) were not stimulated by the analogs, which are responsible for somewhat different intensity patterns among the studied drugs.

Sequence Specificity of Poison Interactions with the Cleavable Complex—Statistical analyses of drug-specific cleavage site sequences were performed for *m*-AMSA, 9-IHA, and 1-IHA. Even though the new analogs were less active than *m*-AMSA, we could collect enough cleavage sites for 9-IHA and 1-IHA to evaluate base sequences with statistical tests (Table I and Fig. 5). In the same DNA fragments, more than 150 sites stimulated by *m*-AMSA were also collected, and the results confirmed a strong preference for adenine at +1 positions (2, 17). In the case of 9-IHA, we found that the highest base preference was present at position +1 for adenine, and in addition a preference for cytosines at position −1. Previously, a secondary preference for thymines was observed at position −1 in the case of *m*-AMSA (2). In the case of 1-IHA, no statistically relevant preference has been observed at positions −1 and +1, and an exclusion of guanines was noticed at position +6 only (Fig. 5 and Table I).

These findings demonstrated that the main base preference was identical for 9-IHA and *m*-AMSA (A at +1), even though the former but not the latter preferred a cytosine at −1 position. Moreover, since 1-IHA completely lost the base preference found for *m*-AMSA and bisantrene, our data indicated a substantial modification in recognition of topoisomerase II-DNA covalent complexes by 1-IHA as compared with the other congeners.

Thermodynamics of DNA Binding—All test compounds (Fig. 1) were able to interact effectively with naked DNA as shown by spectrophotometric and fluorometric determinations of binding parameters at physiological conditions (Table II). The K_i values for 1,4-IHA could not be determined since the drug-DNA complex tended to precipitate even at low binding ratios (not shown), demonstrating an outstandingly high binding constant. In agreement with published reports (3, 27, 28), *m*-AMSA and bisantrene showed a modest and very large affinity for DNA, respectively (Table II). The new bisantrene analogs, bearing a side chain only, had intermediate values of DNA binding affinity. A comparison of aza-9-IHA with *m*-AMSA,

FIG. 3. **DNA cleavage intensity patterns by murine native topoisomerase II.** SV40 DNA fragments were reacted with murine topoisomerase II with or without drugs for 20 min at 37 °C, stopped with SDS and proteinase K, and then analyzed on a 8% polyacrylamide sequencing gel. Lanes are as follows: *C*, control DNA, and *T*, topoisomerase II without drugs. Drug-treated samples are as indicated *above* each lane. *A*, *numbers* indicate selected cleavage sites; an *asterisk* indicates a weak cleavage site common to 1-IHA and *m*-AMSA. *B*, *arrowheads* indicate sites of cleavage stimulated by the studied compounds.
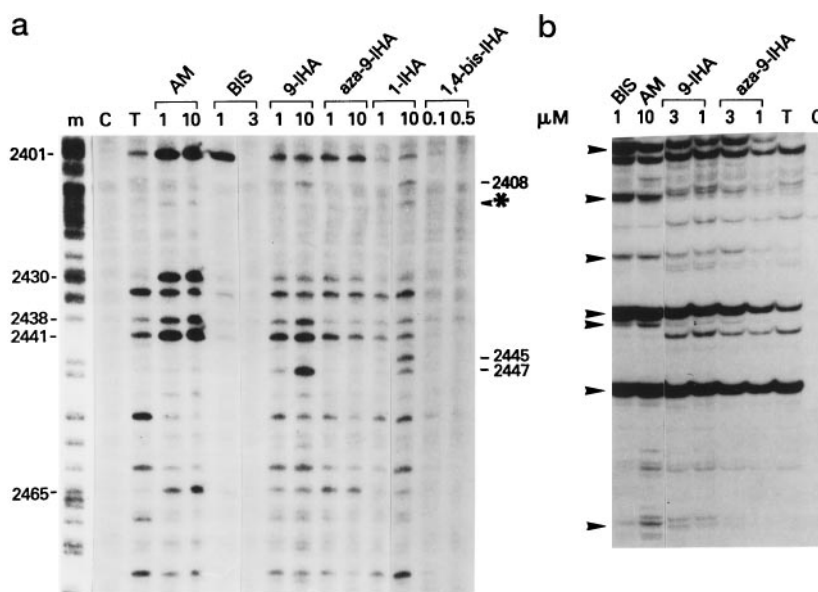
having the same planar portion, indicates that the dihydroimidazolyl hydrazone side chain generated remarkably stronger interactions with the nucleic acid than the methane sulfone *m*-anisidide group (Table II). The location of the side chain on the planar ring system plays a role in directing complex formation, since 1-IHA had a 3-fold lower constant than the 9-substituted isomers. The exclusion parameter *n* was close to 2 base pairs for all 9-substituted compounds, in agreement with an intercalative process of binding. On the other hand a considerably lower *n* value was found for 1-IHA (Table II), suggesting an important non-intercalative component to the binding process.

Molecular Drug Conformations: Computer Simulation and NMR Studies—Structural information about the orientation of the side chain groups relative to the planar ring system was experimentally obtained by NOE spectra of 9- and 1-IHA relative to irradiation of the iminic protons (Fig. 6*A*). Both compounds gave intense signals in the NOE difference spectra. The data for 9-IHA gave 26.9% enhancement for protons H-1 and H-8 (exhibiting the same chemical shift) of the anthracene ring, whereas enhancements observed in the presence of 1-IHA were 11.6% for H-9 and 14.9% for H-2 referred to the same ring system. These data are consistent with a relatively free rotation of the side chain around the $C_{aromatic}$-C_{iminic} bond.

In addition to bisantrene and *m*-AMSA (17), we have investigated low energy conformations of the IHA drugs by computer-aided modeling techniques to identify the structural determinants of the drug sequence-specific action. Each structure was first energy-minimized to find the most stable conformations, as obtained from a systematic conformational analysis. For each compound, structures within 3 kcal/mol of the minimum energy were considered, since most biologically relevant conformations are normally expected to be included in such an energy range. As previously reported (17), and consistent with the nuclear Overhauser experiments (Fig. 6*A*), the dihydroimidazolyl hydrazone side chains of bisantrene were characterized by a high degree of conformational freedom, and low energy dynamic structures of the drug displayed two symmetric sets of chain space occupancy with respect to the plane of the aromatic moiety (not shown). The most stable structure *in vacuum* was defined by the following values of the adjacent dihedral angles starting from one of the imidazole nitrogens: N-C-N-N = 150°; C-N-N-C = 110°; N-N-C-C = −140°; N-C-C=C = −64°.
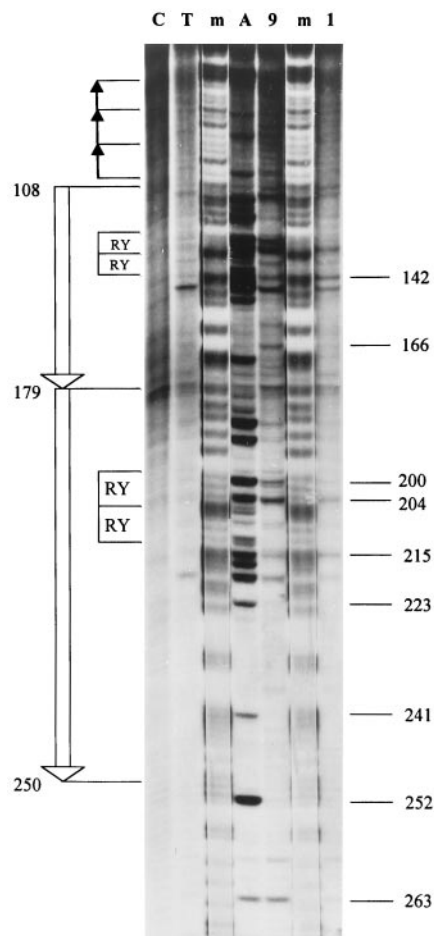

FIG. 4. **Cleavage patterns by human topoisomerase IIα at the replication origin region of simian virus 40.** An SV40 DNA fragment was labeled at the *Ban*I site, and cleavage reactions were performed as described in the legend to Fig. 3. Drugs were used at 10 μM. *Numbers* on the *right* indicate cleavage sites. Symbols are as follows: *upward arrows*, 21-base pair repeats; *RY*, alternating purine/pyrimidine sequences; *downward arrows*, 72-base pair repeats. *Numbers* correspond to SV40 genomic positions. Lanes are as follows: *C*, control DNA; *T*, enzyme alone; *m*, purine markers; *A*, *m*-AMSA; *9*, 9-IHA; and *1*, 1-IHA. The purine marker lanes are from a 5-fold less exposed autoradiography.

TABLE I

Base frequencies (%) at the sites of topoisomerase II DNA cleavage stimulated by the indicated poison

Site sequences were aligned with respect to the observed cleaved phosphodiester bond, which is between nucleotides −1 and +1. The numbers of cleavage sites were 66 and 37 for 9-IHA and 1-IHA, respectively; for *m*-AMSA, the statistical data of the analysis of 48 strong sites are reported. Base frequencies in SV40 DNA are 29.6% of A and T, and 20.4% of G and C. In bold, statistically significant high frequencies (11, 23).

|						Position from the cleavage site								
	−5	−4	−3	−2	−1	+1	+2	+3	+4	+5	+6	+7	+8	+9
m-AMSA														
A	16.7	22.9	41.7	39.6	31.3	**52.1**	37.5	16.7	16.7	22.9	35.4	25.0	39.6	29.2
G	31.3	18.8	16.7	31.3	18.8	8.3	29.2	27.1	18.8	31.3	10.4	14.6	6.3	25.0
C	18.8	25.0	6.3	6.3	20.8	14.6	18.8	29.2	16.7	16.7	29.2	25.0	25.0	18.8
T	33.3	33.3	35.4	22.9	29.2	25.0	14.6	27.1	**47.9**	29.2	25.0	35.4	29.2	27.1
9-IHA														
A	24.2	36.4	34.8	34.8	22.7	**45.5**	33.3	13.6	27.3	33.3	25.8	30.3	31.8	27.3
G	16.7	19.7	21.2	31.8	18.2	16.7	24.2	24.2	13.6	22.7	13.6	7.6	7.6	19.7
C	28.8	19.7	15.2	12.1	**33.3**	21.2	19.7	24.2	30.3	21.2	24.2	28.8	30.3	21.2
T	30.3	24.2	28.8	21.2	25.8	16.7	22.7	37.9	28.8	22.7	36.4	33.3	30.3	31.8
1-IHA														
A	24.3	27.0	43.2	35.1	24.3	43.2	32.4	18.9	37.8	27.0	16.2	29.7	32.4	16.2
G	21.6	24.3	16.2	32.4	18.9	24.3	21.6	27.0	10.8	27.0	13.5	2.7	8.1	29.7
C	21.6	27.0	5.4	10.8	32.4	13.5	8.1	21.6	29.7	13.5	35.1	21.6	32.4	21.6
T	32.4	21.6	35.1	21.6	24.3	18.9	37.8	32.4	21.6	32.4	35.1	45.9	27.0	32.4
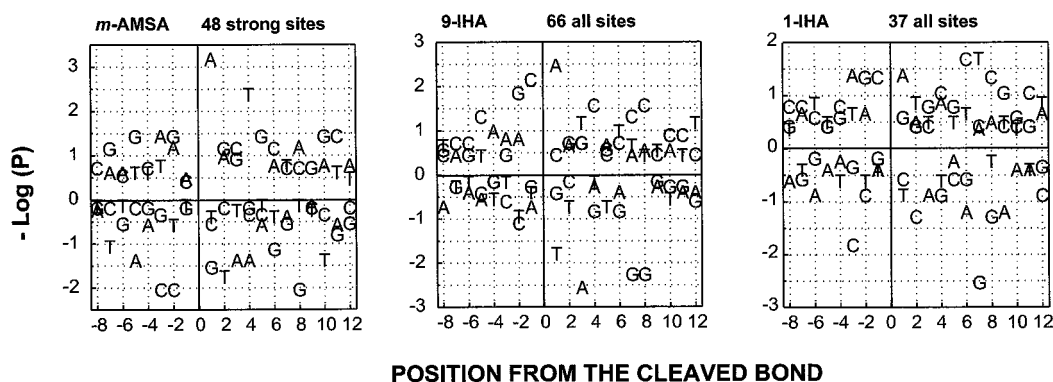
FIG. 5. **Base preferences at the site of poison-stimulated DNA cleavage.** Nucleotide sequences of sites stimulated by *m*-AMSA (*left*), 9-IHA (*middle*), and 1-IHA (*right*) were collected and analyzed by statistical tests (11, 23). −*Log(p)* values indicate the chance of observing that deviation or more as either excess or deficiency (above or below the *zero line,* respectively) relative to the expected frequency of each base (G = C = 20.6%; A = T 29.4%).

TABLE II

Thermodynamic properties of binding to calf thymus DNA by the test compounds

DNA binding affinity constants were determined in 10 mM Tris-HCl, pH 7.0, 1 mM EDTA, 0.15 M NaCl at 25 °C.

Compound	$K_i \times 10^4$ (M^{-1})	n (bases)
1-IHA	3.20 ± 0.1	2.6 ± 0.3
9-IHA	11.1 ± 0.34	4.2 ± 0.1
Aza-9-IHA	9.28 ± 0.23	4.5 ± 0.2
m-AMSA	0.30 ± 0.02	3.5 ± 0.3
Bisantrene	217 ± 11	4.5 ± 0.2

Steric and Electrostatic Alignment (SEA) of IHA Congeners— For steric and electrostatic analyses, we used optimized geometries and atomic charges obtained for the test compounds from *ab initio* calculations. In addition to bisantrene, 9-IHA and 1-IHA were used to define the physicochemical properties of monosubstituted isomers. As it could be anticipated, the similarity between 9-IHA and bisantrene is very high, exhibiting an almost complete steric and electronic matching (not shown). This clearly suggested a very similar fashion of drug-receptor interaction for the two compounds. On the contrary, the three-

dimensional similarity analysis based on the steric and electronic properties of 1-IHA and 9-IHA gave a poor correlation coefficient (0.54). This value fully agreed with the low similitude shown by the optimized overlapping of all stable conformations of the two compounds (Fig. 7). In fact, to achieve the best balance between common space occupancy and electrostatic potential, the planar moieties must be tilted and shifted one with reference to the other, so that side chain groups are forced to occupy distinct regions in space (Fig. 7). The different superimposition between 1-IHA and 9-IHA was corroborated with comparative charge localization analysis. As shown in Fig. 6B, the shift of the side chain from 9 to 1 position of the anthracene moiety completely modified the electronic charge distribution around the two molecules. Consequently, the dipole moments of the two congeners are also different (Fig. 6B), indicating that the topology of the electrostatic potential may represent an important factor in the molecular recognition process. Taken together, our results indicate that steric features and electrostatic potential fields of minimum energy conformations common to bisantrene, *m*-AMSA, and the studied 9-IHA analogs are not shared by the structural isomer 1-IHA.
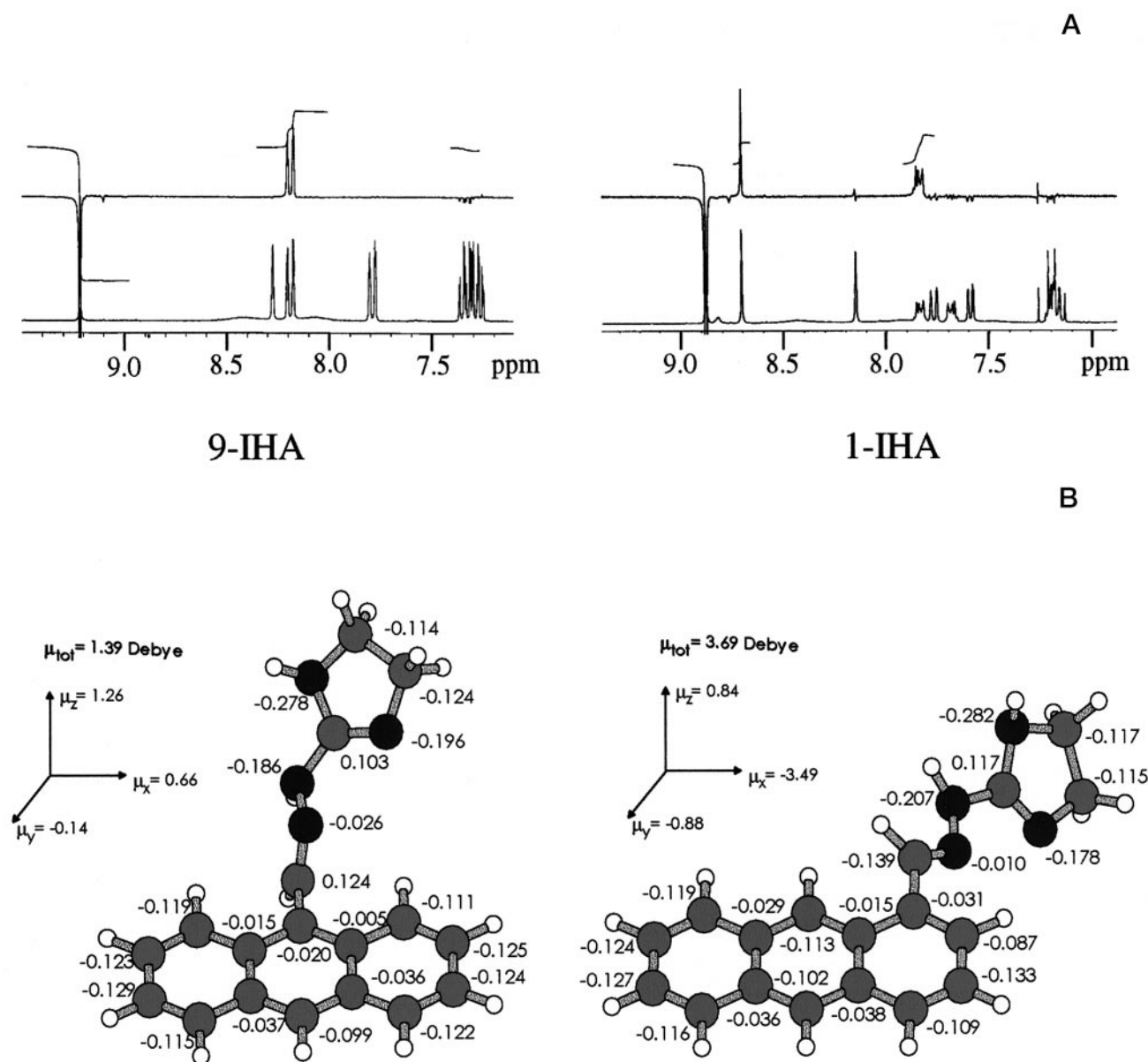
FIG. 6. **Conformational analyses of 1-IHA and 9-IHA.** *A*, NMR examination of the side chain orientation relative to the aromatic ring system of drugs in solution. ¹H NMR (*bottom*) and NOE difference spectra (*top*) of the aromatic protons of 9-IHA (*left*) and 1-IHA (*right*). *B*, atomic charges and vector composition of electric dipole moment of the studied IHA agents. The values were obtained by using an *ab initio* RHF/3–21G(*) methodology for the model of 1-IHA and 9-IHA structures. Atoms are shown as *circles*: *dark gray,* nitrogen; *light gray*, carbon; and *white*, hydrogen.

This is expected to modify the recognition of the receptor site by 1-IHA.

DISCUSSION

The present investigation on IHA congeners, the design of which was prompted by earlier molecular modeling studies (17), definitely demonstrates that, in a homogeneous series of compounds, alterations of the shape and electron density of the drug molecule markedly affect the sequence-specific poison interaction with topoisomerase II-DNA complexes. Thus, this result strongly supports the idea that the relative position of putative DNA- and enzyme-binding domains plays a key role in determining the sequence position specificity of topoisomerase II poisons (2).

The NOE results presented in Fig. 6*A* confirm the possibility of free rotation of the side chain groups with reference to the planar anthracene moiety. Hence, a number of conformations characterized by similar energies are available for the molecule to interact at the receptor site. This is confirmed by the theo-

retical *ab initio* analysis, giving small energy gaps between stable conformations, the limiting situations being represented by a completely planar arrangement or a perpendicular arrangement of the imidazolyl hydrazine group *versus* the anthracene group. The SEA analysis comparing the complete range of stable conformations of 9-IHA with the complete set of stable conformations of 1-IHA was not able to find a satisfactory alignment within the two sets of conformers. This confirms that 1-IHA and 9-IHA correspond to distinct pharmacophores. This is further emphasized by the fact that the observed changes in electrostatic potential are not a consequence of the drug conformation but a result of the 9 → 1 shift of the side chain group (Fig. 6*B*).

Our data establish that one side chain of bisantrene is sufficient to grant poisoning activity to the compound since 9-IHA could stimulate even higher levels of topoisomerase II DNA cleavage than bisantrene, although the DNA affinity was maximum when two dihydroimidazolyl chains were present. In-
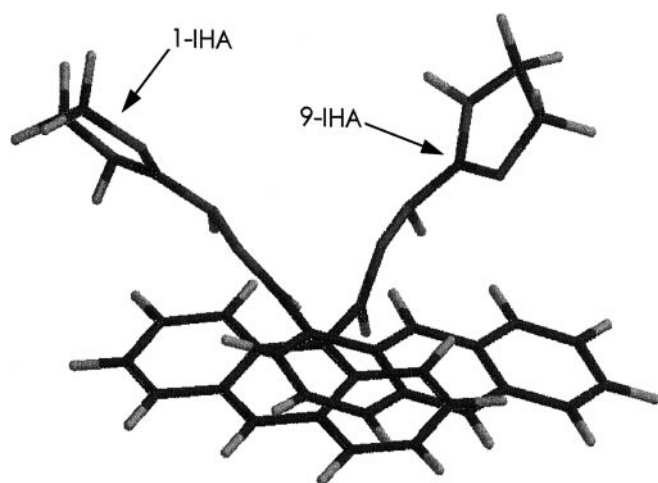
FIG. 7. **Steric and electronic alignment (SEA) analysis of the most probable overlapping between 9-IHA and 1-IHA.** The correlation coefficient is 0.54 (see "Experimental Procedures" for details).

deed, the binding affinity dropped about 20-fold by removing one chain and 30-fold further when replacing the bisantrene chain with the *m*-AMSA side group. On the other hand, the substitution of the anthracene ring with the acridine planar moiety in aza-9-IHA did not appreciably alter the binding properties. This indicates that the aza substitution at the central ring does not play an important role in the energy balance of DNA-drug complex formation. Only a slight decrease is observed when shifting the chain from position 9 to position 1; hence, the location of side groups in the IHA/amsacrine family does not significantly affect DNA affinity.

The effect of poison substituents on DNA cleavage levels cannot be determined by a simple comparison of cleavage efficiencies. In fact, as mentioned above, DNA binding constants of the studied compounds were markedly different, and it is well known that a strong interaction with free DNA by intercalating agents can fully prevent enzyme binding to the nucleic acid and therefore enzyme-mediated DNA cleavage (2, 5, 6). Cleavage levels stimulated by bisantrene were low, whereas they were prominent when using the weak binder *m*-AMSA; IHA congeners had intermediate effects, consistent with their intermediate K_i values. Since the relative efficiencies in DNA cleavage stimulation were inversely correlated to nucleic acid binding constants for this series of compounds, the extent of cleavage stimulation could be mostly determined by the DNA binding affinity. Indeed, cleavage suppressive effects shown by 1,4-IHA well paralleled its very high DNA binding activity, which even prevented drug dissociation from the complex. The only compounds having essentially the same affinity for DNA were 9-IHA and aza-9-IHA. In this case, it is safe to conclude that the C $\rightarrow$ N bioisosteric substitution at the central ring was primarily responsible for the reduced cleavage activity. In agreement with this result, a double C $\rightarrow$ N bioisosteric substitution in anthracenediones (including mitoxantrone) has been shown to abolish topoisomerase poisoning activity (29).

The statistical analysis documented that an adenine(+1) requirement for cleavage stimulation is shared by bisantrene, *m*-AMSA, 9-IHA, and the hybrid drug, aza-9-IHA (data not shown). Hence, these agents likely belong to a very similar pharmacophore class and interact similarly in the ternary DNA-poison-topoisomerase II complex. In total agreement with this hypothesis, the above drugs were characterized by a similar electron density and spatial relation of drug moieties as determined by the SEA analysis of drug conformations obtained by *ab initio* theoretical calculations. In the case of 1-IHA, which had the side chain shifted to a lateral ring, radical changes were instead observed; the compound was still able to poison topoisomerase II; however, cleavage was no longer preferentially stimulated at m-AMSA sites. Therefore, we may conclude that 1-IHA cannot share the same pharmacophore as the other congeners of the bisantrene/*m*-AMSA family. Consistently, the molecular modeling analysis showed that 1-IHA and 9-IHA were rather different molecules, since a similarity parameter of 0.54 indicated that the two compounds were not more alike than any two of the vast majority of chemically unrelated DNA-interacting agents.

At this time, we do not have direct evidence of the relative position of the 9- and 1-IHA structures within the DNA-enzyme covalent complex; nevertheless, we can reasonably argue that the 9-IHA derivatives are present at the enzyme/DNA interface specifically interacting with the adenine at the cleavage site in a fashion similar to bisantrene and *m*-AMSA (2, 17). A simple isomerization in the IHA structure causes dramatic modifications in the sequence specificity of poison-stimulated topoisomerase II DNA cleavage. Thus, the present results strongly support the hypothesis that only compounds sharing defined steric and electronic features can trap the enzyme at the same DNA sites, suggesting a similar fit into the receptor site (17). Taken individually, the chemical identity of the functional groups of 1- and 9-IHA would allow the same stabilizing interactions to occur with the receptor site. However, the different reciprocal location of ring system and side chain impairs the contextual onset of the key contacts with the protein and nucleic acid partners in the covalent topoisomerase II-DNA complex. This strengthens the concept of a cooperation between (at least) two pharmacophoric domains in eliciting specific target recognition and, hence, in affecting drug activity.

In conclusion, molecular modeling of poison molecules, and possibly poison-receptor interactions, may be powerful tools in drug discovery when combined with experimental molecular analyses of topoisomerase-dependent DNA cleaving effects. The complete definition of the diverse pharmacophores of topoisomerase II poisons will certainly be of value for the design of new agents more effective in the treatment of human cancers.

REFERENCES

1. Palumbo, M. (1998) *Advances in DNA Sequence-specific Agents 3*, Jai Press Inc., Greenwhich, CT
2. Capranico, G., Binaschi, M., Borgnetto, M. E., Zunino, F., and Palumbo, M. (1997) *Trends Pharmacol. Sci.* **18,** 303–346
3. Baguley, B. C. (1991) *Anti-Cancer Drug Des.* **6,** 1–35
4. Bailly, C., Denny, W. A., and Waring, M. J. (1996) *Anti-Cancer Drug Des.* **11,** 611–624
5. Pommier, Y. (1997) in *Cancer Therapeutics: Experimental and Clinical Agents* (Teicher, B. A., ed) pp. 153–174, Humana Press Inc., Totowa, NJ
6. Liu, L. F. (1989) *Annu. Rev. Biochem.* **58,** 351–375
7. Froelich-Ammon, S. J., and Osheroff, N. (1995) *J. Biol. Chem.* **270,** 21429–21432
8. Wang, J. C. (1996) *Annu. Rev. Biochem.* **65,** 635–692
9. Watt, P. M., and Hickson, I. D. (1994) *Biochem. J.* **303,** 681–695
10. Osheroff, N., Zechiedrich, E. L., and Gale, K. C. (1991) *BioEssays* **13,** 269–273
11. Capranico, G., Kohn, K. W., and Pommier, Y. (1990) *Nucleic Acids Res.* **18,** 6611–6619
12. Pommier, Y., Capranico, G., Orr, A., and Kohn, K. W. (1991) *J. Mol. Biol.* **222,** 909–924
13. Freudenreich, C. H., and Kreuzer, K. N. (1994) *Proc. Natl. Acad. Sci. U. S. A.* **91,** 11007–11011
14. Jaxel, C., Capranico, G., Kerrigan, D., Kohn, K. W., and Pommier, Y. (1991) *J. Biol. Chem.* **266,** 20418–20423
15. Pommier, Y., Kohlhagen, G., Kohn, K. W., Leteurtre, F., Wani, M. C., and Wall, M. E. (1995) *Proc. Natl. Acad. Sci. U. S. A.* **92,** 8861–8865
16. Macdonald, T. L., Lehnert, E. K., Loper, J. T., Chow, K.-C., and Ross, W. E. (1991) in *DNA Topoisomerases in Cancer* (Potmesil, M., and Kohn, K. W., eds) pp. 199–214, Oxford University Press, New York

17. Capranico, G., Palumbo, M., Tinelli, S., Mabilia, M., Pozzan, A., and Zunino, F. (1994) *J. Mol. Biol.* **235,** 1218–1230
18. Zagotto, G., Oliva, A., Guano, F., Menta, E., Capranico, G., and Palumbo, M. (1998) *Bioorg. & Med. Chem. Lett.* **8,** 121–126
19. De Isabella, P., Capranico, G., Binaschi, M., Tinelli, S., and Zunino, F. (1990) *Mol. Pharmacol.* **37,** 11–16
20. Cornarotti, M., Tinelli, S., Willmore, E., Zunino, F., Fisher, L. M., Austin, C. A., and Capranico, G. (1996) *Mol. Pharmacol.* **50,** 1463–1471
21. McGhee, J. D., and von Hippel, P. H. (1974) *J. Mol. Biol.* **86,** 469–489
22. De Isabella, P., Zunino, F., and Capranico, G. (1995) *Nucleic Acids Res.* **23,** 223–229
23. Pommier, Y., Capranico, G., Orr, A., and Kohn, K. W. (1991) *Nucleic Acids Res.* **19,** 5973–5980
24. Hehre, W. J., Radom, L., Schleyer, P. V. R., and Pople, J. A. (1986) *Ab Initio Molecular Orbital Theory*, John Wiley & Sons, New York
25. Martin, Y. C., Bures, M. G., and Willet, P. (1990) in *Reviews in Computational Chemistry* (Lipkowitz, K. B., and Boyd, D. B., eds) p. 213, VCH Publisher, Inc., New York
26. Dewar, M. J. S., Zoebisch, E. G., Healy, E. F., and Stewart, J. J. P. (1985) *J. Am. Chem. Soc.* **107,** 3902–3910
27. Wunz, T. P., Craven, M. T., Karol, M. D., Hill, G. C., and Remers, W. A. (1990) *J. Med. Chem.* **33,** 1549–1553
28. Chen, K.-X., Gresh, N., and Pullman, B. (1988) *Nucleic Acids Res.* **16,** 3061–3073
29. De Isabella, P., Palumbo, M., Sissi, C., Capranico, G., Carenini, N., Menta, E., Oliva, A., Spinelli, S., Krapcho, A. P., Giuliani, F. C., and Zunino, F. (1995) *Mol. Pharmacol.* **48,** 30–38

Mapping Drug Interactions at the Covalent Topoisomerase II-DNA Complex by Bisantrene/Amsacrine Congeners

Giovanni Capranico, Fulvio Guano, Stefano Moro, Giuseppe Zagotto, Claudia Sissi, Barbara Gatto, Franco Zunino, Ernesto Menta and Manlio Palumbo